World Journal of Advanced Engineering Technology and Sciences
eISSN: 2582-8266
Cross Ref DOI: 10.30574/wjaets
Journal homepage: https://wjaets.com/

(RESEARCH ARTICLE)

Check for updates

Application of the Taguchi and ANOVA methods to optimize high-energy ball milling parameters for dislocation density of TiO_2 powder

Maya Radune [1,*], Svetlana Lugovskoy [2], Yaniv Knop [1] and Barbara Kazanski [3]

[1] *Civil Engineering Department, Ariel University, Ariel, Kiryat Hamada, 40700, Israel.*
[2] *Chemical Engineering Department, Ariel University, Ariel, Kiryat Hamada, 40700, Israel.*
[3] *Materials Engineering Department, Azrieli College of Engineering, Jerusalem, 91035000, Israel.*

World Journal of Advanced Engineering Technology and Sciences, 2025, 15(01), 1589-1603

Publication history: Received on 23 February 2025; revised on 07 April 2025; accepted on 09 April 2025

Article DOI: https://doi.org/10.30574/wjaets.2025.15.1.0100

Abstract

Due to its particular properties, titanium dioxide (TiO_2) has been widely used in industry. In this study, the high-energy ball milling (HEBM) parameters, including milling time (MT), ball-to-powder weight ratio (BPWR), and milling speed (MS), have been optimized using the Taguchi method.

TiO_2 dislocation density (DD) was used to estimate the effect of the HEBM. The experiment was applied using the $L16(4^3)$ orthogonal array (OA). The as-received and milled powders were characterized by X-ray diffraction (XRD). The DD, determined by the Williamson-Hall (W-H) method in XRD patterns, varied between $0.02 \cdot 10^{-2}$ – $8.26 \cdot 10^{-2}$ lines/nm^2 depending on the HEBM conditions. The optimum milling parameter combination was determined by analysis of signal-to-noise (S/N) ratio. Based on the S/N ratio analysis, optimal HEBM conditions were found at MT 50h, MS 600rpm, BPWR 50:1. The analysis of variance (ANOVA) was used to find the significance and percentage of contribution of each milling parameter. Statistical analysis by S/N and ANOVA established that the MT was the most effective parameter, followed by MS and BPWR. The results of the parameter optimization experiments were validated by a confirmation test with a 90% confidence level.

Keywords: High-Energy Ball Milling; Titanium Dioxide Powder; Taguchi's Technique; ANOVA; Dislocation Density

1. Introduction

Concrete, a foundational material in modern construction, constantly undergoes innovation to meet the demands of sustainable infrastructure and environmental responsibility [1]. The integration of nanotechnology into concrete admixtures presents a promising approach to enhance its mechanical properties and functionality [2–5]. Among the great number of nanomaterials, titanium dioxide (TiO_2) nanoparticles exhibit exceptional promise due to their high chemical stability, photocatalytic activity, and mechanical reinforcement capabilities [6]. Several studies have investigated the influence of TiO_2 nanoparticles on concrete properties. They found that the addition of TiO_2 nanoparticles improved the concrete's compressive, flexural and split tensile strengths [7], enhanced its resistance to sulfate attack [8], and hindered degradation of concrete surfaces by organic contaminants and nitrogen oxides (NO_X) [9, 10].

A variety of ways have been reported to synthesize TiO_2 nanoparticles, such as sol-gel synthesis [11], hydrothermal methods [12], chemical vapor deposition [13], and high-energy ball milling (HEBM) [14]. The conventional methods predominantly include multi-step procedures, demand the utilization of toxic metal–organic precursors, and require expensive equipment. Also, long processing times are required, which is detrimental to industrial fabrication purposes [15]. HEBM has the advantages of being a simple process, relatively inexpensive to produce, easily scaled up to large quantities, and

* Corresponding author: Maya *Radune*.

environmentally friendly [16]. It provides a high-energy input to the system which leads to a high degree of milling intensity, resulting in the formation of fine and homogeneous nanocrystalline structures [17]. The use of HEBM also allows control of the crystal structures, specific surface area, crystallite size, particle size, and crystal defects, all of which are crucial in determining the physical and chemical properties of TiO_2 [18–20].

Although this preparation route is practically very simple, the process is complex and depends on many factors that affect the physical and chemical properties of the milled powder: the precise dynamic conditions, temperature and nature of the milling tools, MS, size of balls, BPWR, milling medium, MT, etc. [21]. To find the best parameters in the HEBM process of TiO_2, a large number of experiments are required. The Taguchi technique, one among several experimental designs, was chosen due to its simplicity, efficiency and systematic approach in determining the optimal parameters in a manufacturing process [14, 22, 23]. As a result, this method reduces the number of optimization experiments needed [16, 24].

Dislocations are the most important structural component affecting the mechanical properties of materials [25]. Consequently, it is necessary to gain an in-depth understanding of the evolution of dislocation density (DD) during the HEBM process. Such an understanding could be effective in developing the properties of concrete that includes nanosized TiO_2 particles. To the best of our knowledge, there is no information about the influence of HEBM on the DD of TiO_2.

In this study, we applied the Taguchi experimental design and the signal-to-noise (S/N) ratio in HEBM experiments, which were performed on the $L_{16}(4^3)$ orthogonal array (OA). MS, MT and BPWR were selected as control parameters, and each was applied at four levels. Analysis of variance (ANOVA) was used to determine the percentage effects of the various milling parameters.

2. Materials and Methods

High-quality TiO_2 powder (min. 99.9% purity, Sigma Aldrich) was utilized as starting material. The raw TiO_2 particles were micron size and irregular in shape. The HEBM of the TiO_2 powder was accomplished in a planetary ball mill (Retsch PM 100, Germany), with vials of 250ml volume and balls (10mm diameter) made of chromium-hardened steel. The milling was performed at room temperature for the different milling parameters (Table 1).

The structural parameters and phase composition of the initial and milled powders were determined by X-ray diffraction (XRD) using a Panalytical Pert Pro X-ray diffractometer with CuK_α radiation (λ=0.154 nm), operating at 40 kV and 40 mA. Data collection was performed by step scanning of the specimen over the $2\theta : 20 - 70^\circ$ angular range, in steps of 0.05° with 3 sec per step. The XRD line profile parameters were then fitted with Rietveld refinement, using PANalytical X' Pert High Score Plus v3.0e software. The Taguchi method was used for optimization of the HEBM process parameters. Figure 1 depicts the process optimization through the HEBM technique.

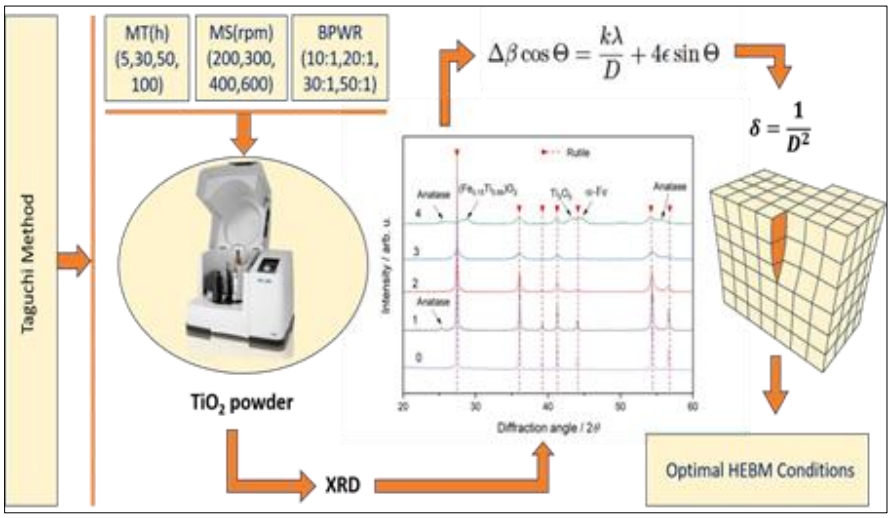

Figure 1 Diagram of DD optimization by HEBM using the Taguchi method

2.1. Determination of structural parameters

The average crystallite size (D) and lattice strain (ϵ) for TiO_2 powder was calculated from a broadening of XRD peaks by the Williamson-Hall (W-H) method [26] using the following equations (Eq. 2.1, 2.2):

$\Delta\beta = \beta_D + \beta_\varepsilon$	(2.1)
$\Delta\beta\cos\theta = \frac{k\lambda}{D} + 4\varepsilon\sin\theta$	(2.2)

where $\Delta\beta$ is full width at half maximum (FWHM), β_D and β_ϵ are the integral breadths dependent on crystallite size and strain effects, respectively, k is the shape factor (~ 0.9), λ is the wave length of X-ray (0.154 nm), Θ is the diffraction angle, and ϵ is strain.

The lattice strain (ϵ) and crystallite size (D) were derived from the slope and the y-intercept of the linear fit, respectively. The value of the crystallite size was used to evaluate the DD (δ) (Eq. 2.3) [27, 28]:

$\delta = \frac{1}{D^2}$	(2.3)

2.2. The Taguchi method

Genichi Taguchi developed a methodology for the application of designed experiments. He proposed that engineering the optimization of a process or product should be carried out in a three-step approach: system design, parameter design, and tolerance design. The parameter design is the key step in the Taguchi method to achieve high quality without increasing cost. Its objectives [29] are to optimize the settings of the process parameter values for improving performance characteristics, and to identify the product parameter values under the optimal process parameter values.

In contrast, classical parameter design, as developed by Fisher [30], is complex and not easy to use. It considers all input parameters at each level, where experimental units take on all possible combinations of these levels. This allows the study of each parameter effect on the response variable: if there are k variable each at n levels, the design has nk runs. Therefore, an experiment involving a significant number of parameters involves prohibitive time and costs.

Taguchi suggested a particular method using the orthogonal array (OA) with a minimal number of experiments that could give complete information on all the factors that affect the outcome. The OA is an experiment matrix organizing the number of experiments and the conditions of each experiment. It is generically called L_n, where n represents the number of experiments to be performed.

Taguchi recommended using a loss function to quantify a design's quality, defining the loss of quality as a cost that increases quadratically with the deviation from the target value. Usually, the quality loss function is divided into three categories: "Nominal is best," "smaller is better," and "larger is better" [31]. "Nominal is best" is used if the objective is to reduce variability around a specific target, "Larger is better" is used if the system is optimized when the response is as large as possible, and "Smaller is better" is used if the system is optimized when the response is as small as possible. The value of the loss function is further transformed into a signal-to-noise (S/N) ratio [32], which is a logarithmic function of the response variable with a different trend depending on the type of response (Eq. 2.4 – 2.6).

"Smaller is better":

$\frac{S}{N_S} = -10\log\left(\frac{1}{n}\sum_{i=1}^{n} y_i^2\right)$	(2.4)

"Larger is better":

$\frac{S}{N_L} = -10\log\left(\frac{1}{n}\sum_{i=1}^{n} \frac{1}{y_i^2}\right)$	(2.5)

"Nominal is best":

$$\frac{S}{N_T} = -10\log\left(\frac{1}{n}\sum_{i=1}^{n}\left(y_i - y_0\right)^2\right) \quad (2.6)$$

where n is the number of experiments in the OA, y_i is the i^{th} measured value, and y_0 is the optimal nominal size.

The S/N ratio for each level of process parameters is computed based on the S/N analysis. Regardless of the category of the performance characteristic, the larger S/N ratio corresponds to the better performance characteristic. Therefore, the optimal level of the process parameters is the level with the highest S/N ratio.

Furthermore, ANOVA is performed to discover which process parameters are statistically significant. With the S/N and ANOVA analyses, the optimal combination of the process parameters can be predicted.

Finally, a confirmation experiment is conducted to verify the optimal process parameters obtained from the parameter design.

The Taguchi methodology includes several steps of planning, conducting, and evaluating the results of a matrix of experiments to determine the best levels of control factors [33]. A flowchart of the various steps of the Taguchi method is depicted in Figure 2.

The aim of this work was to analyze the DD of milled TiO_2 powder in relation to the HEBM parameters by applying the Taguchi method. Three controllable HEBM parameters (MS, BPWR, and MT) were studied. Each factor was applied at four levels (Table 1). The levels of the HEBM parameters were selected based on the literature research [34], [35], [22]. We employed a S/N ratio for the "larger is better" loss function, a statistical ANOVA to test the significance of the effects, and an estimation of DD at optimal conditions, followed by experimental verification.

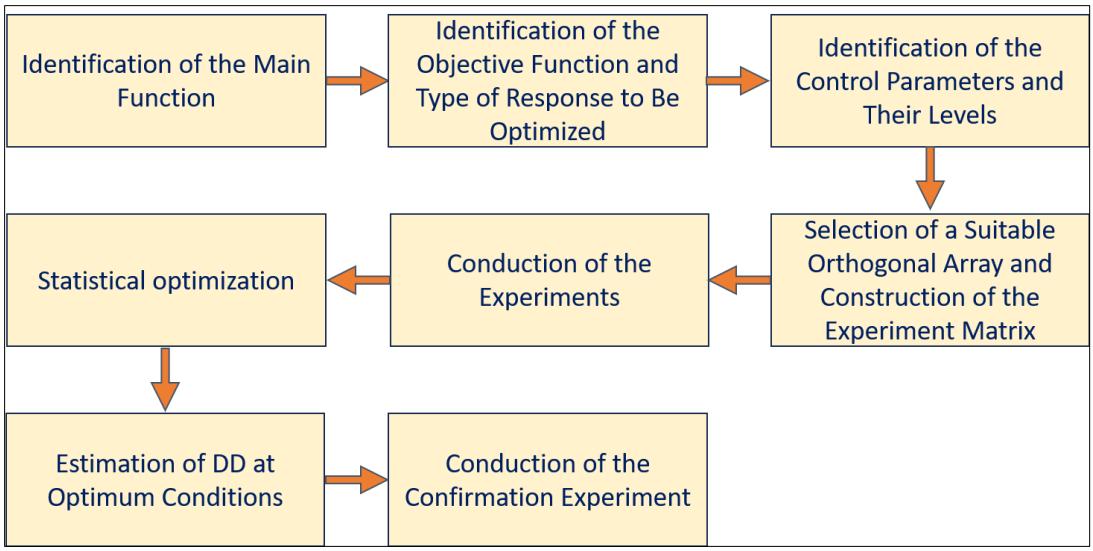

Figure 2 Flow chart of the Taguchi method

3. Results and Discussion

According to the steps in the Taguchi method, a series of HEBM experiments was carried out. Statistical analysis was conducted using Qualitek-4 software. The results are presented in the following subsections.

3.1. Step 1. Identification of the main function

The optimization of DD predictive capability was considered as the main function. Before proceeding, it was necessary to detect all the factors influencing the HEBM, identifying them as signal factors (S) and noise factors (N) [36]. Signal factors are the system control input parameters which can be changed, while noise factors are typically difficult or expensive to control and are assumed to be constant during the experiment. In this work, all the considered factors (MS, MT, and BPWR) were controllable signal factors; none were classified as noise factors.

3.2. Step 2. Identification of the objective function and type of response to be optimized

The DD was chosen as the objective function. Of the three categories of loss function, the "larger is better" response (a variable to be maximized) was chosen for the DD in the analysis of the experimental results (Eq. 2.5). The S/N ratio was also calculated for each level of the parameters. The parameters with the highest S/N ratio were introduced as optimal levels.

3.3. Step 3. Identification of the control parameters and their levels

The HEBM parameters (control parameters) and their levels appear in Table 1.

Table 1 Process Parameters and Their Levels.

Levels	Parameters		
	MT, [h]	MS, [rpm]	BPWR
1	5	200	10:1
2	30	300	20:1
3	50	400	30:1
4	100	600	50:1

3.4. Step 4. Selection of a suitable OA and construction of the experiment matrix

To select an appropriate OA for experiments, the total degrees of freedom (DoF) must be computed. The DoF are defined as the number of comparisons between process parameters that must be made to determine which level is better (Eq. 3.1) [32]:

$$DoF_i = n_i - 1 \quad (3.1)$$

where n_i is the number of factor levels.

Once the required DoF are known, the next step is to select an appropriate OA to fit the specific task. Basically, the DoF for the OA should be greater than or equal to those for the process parameters. In this study, an $L_{16}(4^3)$ OA was used. The experimental layout for the three HEBM parameters using the $L_{16}(4^3)$ OA is shown in Table 2. The OA was chosen from the parameter design OA selector [37].

Table 2 The experimental layout of the $L_{16}(4^3)$ OA

Experiment Number	MT, [h]	MS, [rpm]	BPWR
1	5	200	10:1
2	5	300	20:1
3	5	400	30:1
4	5	600	50:1
5	30	200	20:1
6	30	300	10:1
7	30	400	50:1
8	30	600	30:1
9	50	200	30:1
10	50	300	50:1
11	50	400	10:1
12	50	600	20:1

13	100	200	50:1
14	100	300	30:1
15	100	400	20:1
16	100	600	10:1

3.5. Step 5. Conduction of the experiments

All experiments were performed three times for each of sixteen trial conditions (48 experiments in total), in order to reduce possible biased results. The XRD patterns of all 16 milled TiO_2 powders, according to the conditions in Table 2, are shown in Figure 3.

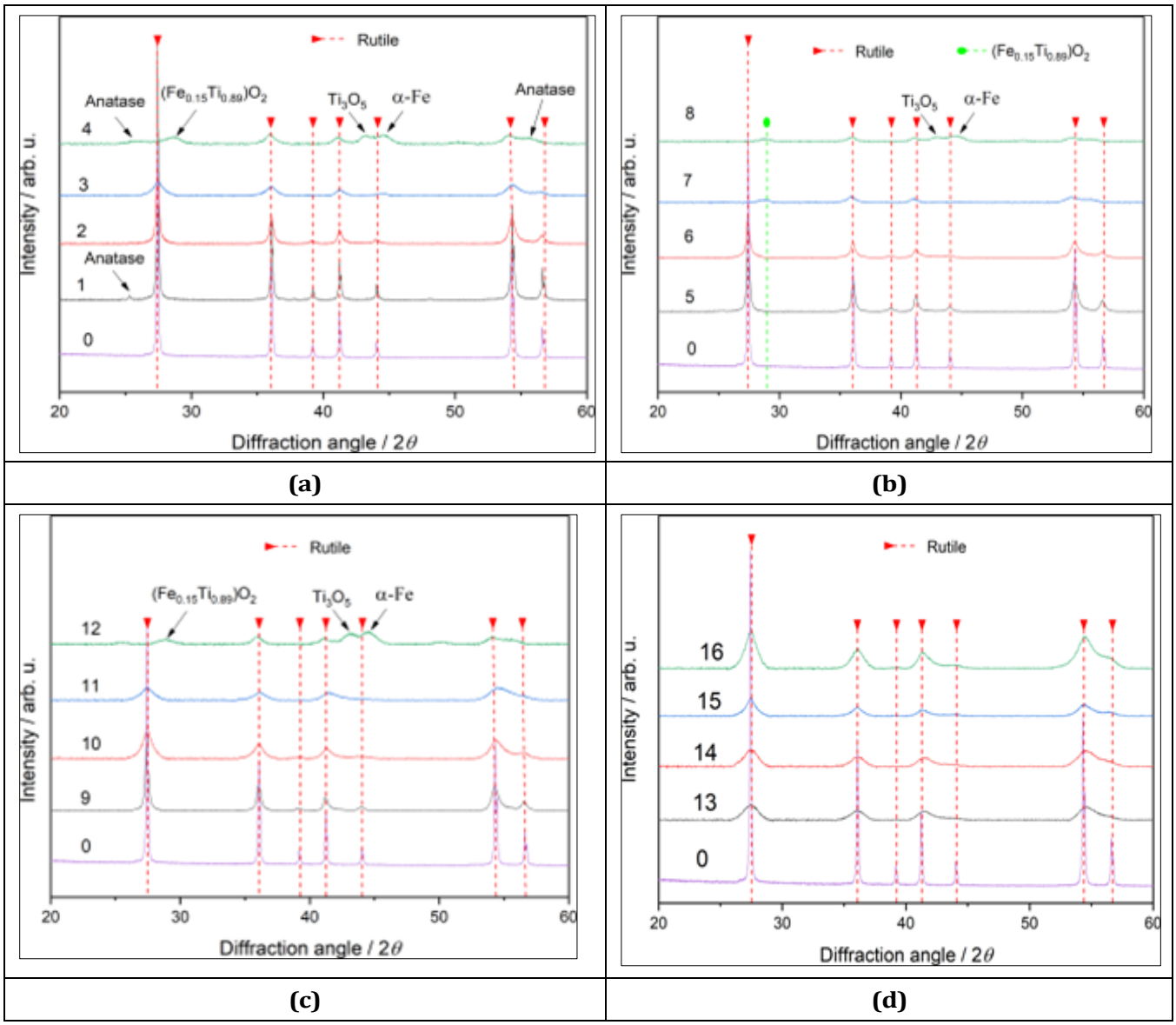

Figure 3 XRD patterns of HEBM TiO_2 powders: (a) 1–4, (b) 5–8, (c) 9–12, (d) 13–16. In each part, the XRD pattern of the initial material (0) is also provided

The effect of HEBM can be clearly traced in the XRD patterns, as evidence of general and significant changes. The intensities of the diffraction peaks of the phases were reduced to different extents, depending on the milling conditions. However, since the Taguchi approach was used, it would be incorrect to ascribe the observed change to the modification of the given condition. Thus, a classical assessment such as decreasing crystallite size with increased milling time, as evidenced in [38–40], could not be applied in this case. All the XRD peaks of the milled TiO_2 samples can be indexed to the

rutile (ICSD:34372), anatase (ICSD:76173), and Ti_3O_5 (ICSD:75194) phases. Additionally, the milled powder contained an impurity fraction of Fe (ICSD:64795) and (Ti, Fe)O (ICSD:283), which originated from the steel grinding medium. The position of these peaks did not change with milling.

The Bragg diffraction peaks were broadened and reduced in intensity, which can be related to the crystallite size reduction and the internal strain in the milling powder. Figure 4 depicts the plot of $\beta \cos \Theta$ versus 4 $\sin \Theta$ for the typical milled TiO_2 powders. The effective strain was calculated from the slope of the linear fit, and the crystallite size was measured by the reciprocal of the intercept.

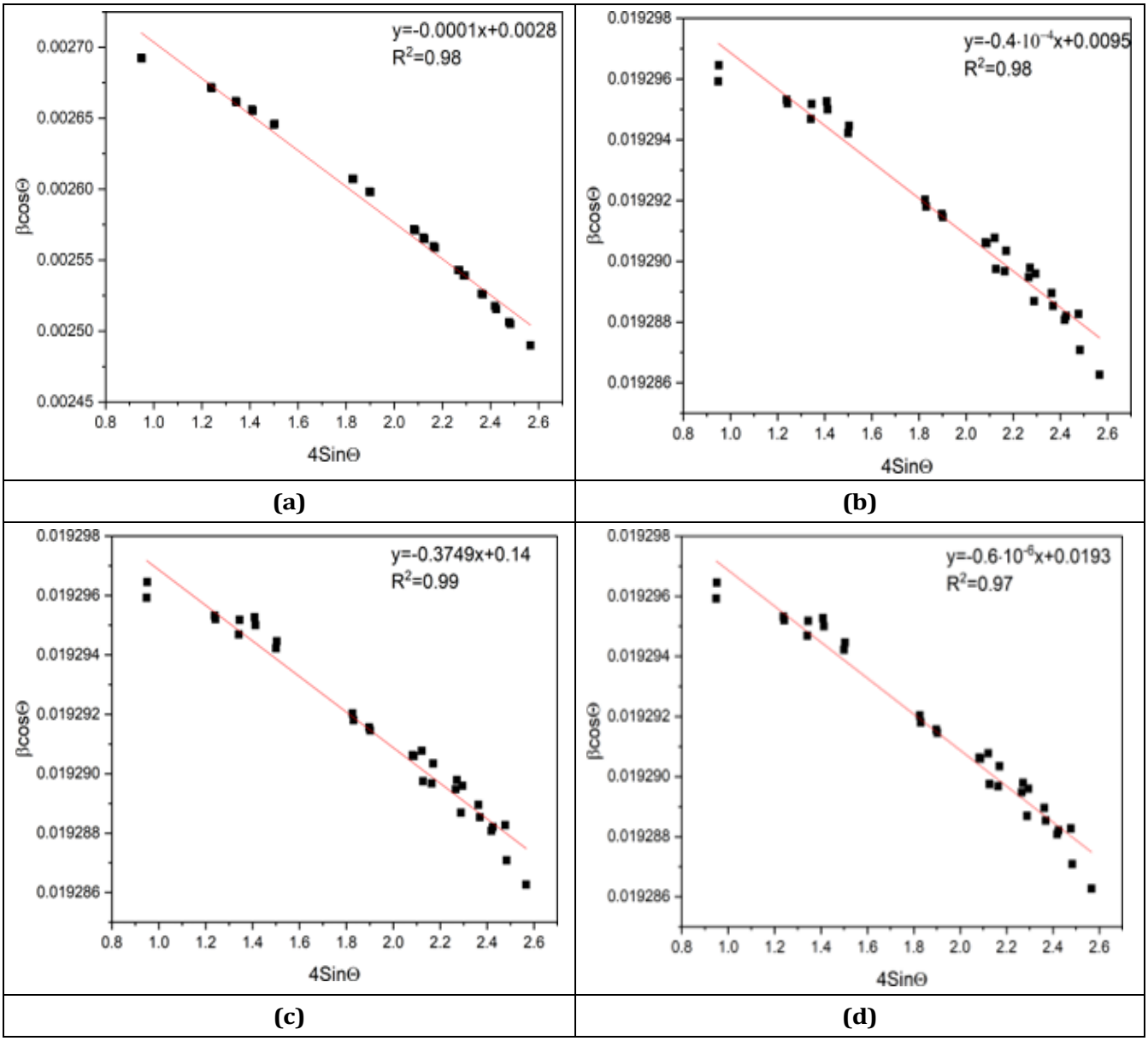

Figure 4 Williamson–Hall plots of milled TiO_2 powders (a): sample 1, (b): sample 6, (c): sample 11, (d): sample 15

The DD was estimated by Eq. 2.3. The average estimated crystallite size, strain and DD for all the samples are displayed in Table 3.

Table 3 The average structural parameters of milled TiO_2 powder and S/N ratios in each experiment of L_{16}

Experiment Number	Crystallite size, nm	DD·10⁻², lines/nm²	Strain·10%	S/N ratio, DB
1	73.7	0.02	0.06	-33.98
2	49.81	0.04	3.26	-27.96
3	8.63	1.34	1.40	2.54
4	6.78	2.18	0.07	6.77
5	29.68	0.11	3.70	-19.17
6	16.10	0.39	0.00	-8.18
7	6.58	2.31	1.34	7.27
8	9.46	1.12	0.84	0.98
9	70.70	0.02	3.49	-33.98
10	6.70	2.23	0.00	6.97
11	3.48	8.26	0.00	18.34
12	6.17	2.63	7.35	8.40
13	3.87	6.68	0.00	16.50
14	3.88	6.64	0.70	16.44
15	8.02	1.55	0.19	5.57
16	6.3	2.52	3.85	8.03

The highest milling efficiency was obtained in Experiments 11, 13, 14 (Figure 5).

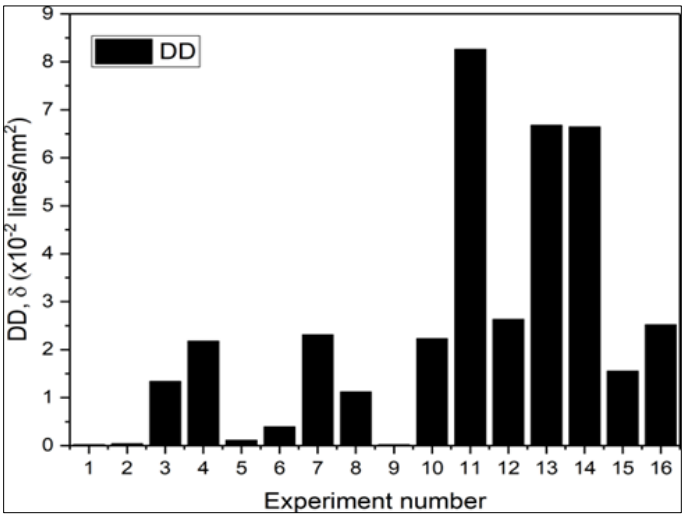

Figure 5 DD of milled $TiO2$ powder. The numbers from 1 to 16 indicate the experiment number

3.6. Step 6. Statistical optimization

The results of the HEBM experiments were studied using the S/N and ANOVA analyses. Based on these analyses, optimal HEBM parameters for DD of milled TiO_2 powder were obtained and verified.

3.6.1. Analysis of the S/N ratio

The experimental results for DD and the corresponding S/N ratio are shown in Table 3. The S/N ratio was computed using Equation 2.5. The differences between the obtained values were strongly dependent on the milling conditions. Since the

experiment design was orthogonal, it was possible to separate out the effect of each milling parameter at different levels [32]. To do this, the mean S/N ratio was determined for each parameter and level. The mean S/N ratio is the average of the S/N ratio for each parameter at different levels [41]. For example, the mean S/N ratio for the MT at levels 1, 2, 3 and 4 can be calculated by averaging the S/N ratios for Experiments 1–4, 5–8, 9-12 and 13–16, respectively. The mean S/N ratio for each level of the other HEBM parameters can be computed in a similar manner. The results are summarized in the S/N response table (Table 4).

Table 4 Response table for TiO_2 DD

Level	MS	MT	BPWR
1	-13.16	-17.66	-3.95
2	-4.77	-3.18	-8.29
3	-0.69	8.43*	-3.50
4	11.63*	6.05	9.38*
Delta Δ	24.79	26.01	17.67
Rank	2	1	3

* Optimum parameter level.

The difference between maximum and minimum S/N ratios (Δ) determines the main effect of the parameter. With greater (Δ) values for a parameter, the effect of the parameter on the process will correspond to a smaller variance in the output, which will generate better performance of the experiment [42]. From the standpoint of the "larger is better" quality characteristic, the MT (Δ = 26.01) had the largest effect on the TiO_2 DD, while BPWR had the smallest effect (Δ = 17.67). A parameter level corresponding to the maximum average S/N ratio is identified as the optimal level for that parameter [43]. Based on the S/N ratio analysis, the optimal conditions for higher TiO_2 DD were: MS_4 (600rpm), MT_3 (50h) and $BPW\ R_4$ (50:1) (Figure 6).

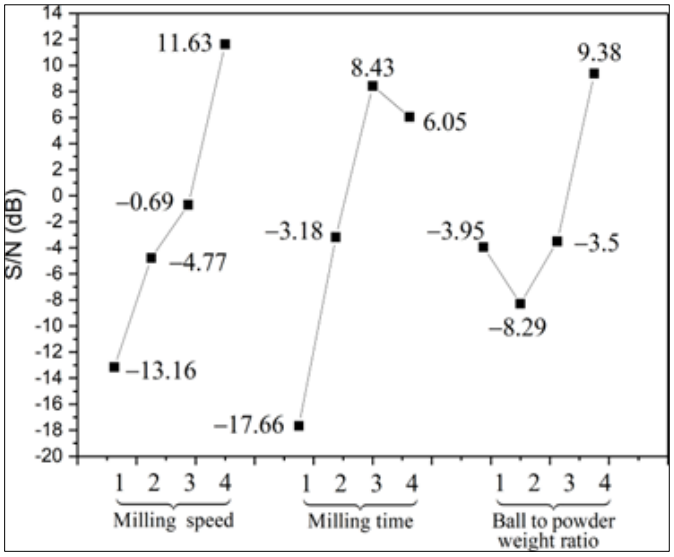

Figure 6 Main effect of process parameters on S/N

3.6.2. Analysis of variance (ANOVA)

The purpose of the ANOVA is to investigate which of the process parameters significantly affects the performance characteristics. This is accomplished by separating the total variability of the S/N ratios, which is measured by the sum of the squared deviations from the total mean of the S/N ratio, into contributions by each of the process parameters and the error. First, the total sum of the squared deviations SS_T from the total mean of the S/N ratio η can be calculated as:

$$SS_T = \sum_{i=1}^{n}\left(\eta_i - \bar{\eta}\right)^2 = \sum_{i=1}^{n}\eta_i^2 - \frac{1}{n}\left[\sum_{i=1}^{n}\eta_i\right]^2 \quad (3.2)$$

where n is the number of experiments in the OA, e.g., n = 16; and η_i is the mean S/N ratio for the i^{th} experiment.

The total sum of the squared deviations SS_T is decomposed into two sources: the sum of the squared deviations SS_P due to each process parameter, and the sum of the squared error SS_e. SS_P can be calculated as:

$$SS_P = \sum_{j=1}^{t}\frac{\left(s\eta_i\right)^2}{t} - \frac{1}{n}\left[\sum_{i=1}^{n}\eta_i\right]^2 \quad (3.3)$$

where p represent one of the experiment parameters, j is the level number of this parameter p, t is the repetition of each level of the parameter p, and $s\eta_j$ is the sum of the S/N ratio involving this parameter p and level j. The sum of squares from error parameters SS_e is

$$SS_e = SS_T - SS_{MT} - SS_{MS} - SS_{BPWR} \quad (3.4)$$

where SS_{MT}, SS_{MS}, SS_{BPWR} are deviations, due to MT, MS, and BPWR, respectively.

The total DoF can be calculated using Equation 3.1, where the DoF of the tested parameter $DoF_P = t - 1$. The variance of the tested parameter is $V_P = SS_P / DoF_P$. Then, the *F*-value for each design parameter is simply the ratio of the mean of the squared deviations to the mean of squared error $F_P = V_P / V_e$. The corrected sum of squares S_P can be calculated as:

$$\hat{S}_P = SS_P - DoF_P \cdot V_e \quad (3.5)$$

The percentage contribution ρ can be calculated as:

$$\rho = \frac{\hat{S}_P}{SS_T} \quad (3.4)$$

Statistically, there is a tool called the F-test, named after Fisher [44], to determine which process parameters have a significant effect on the performance characteristic. In performing the F-test, the mean of the squared deviations SS_m due to each process parameter needs to be calculated. The mean of the squared deviations SS_m is equal to the sum of the squared deviations SS_d divided by the number of DoF associated with the process parameter. Then, the *F*-value for each process parameter is simply a ratio of the mean of the squared deviations SS_m to the mean of the squared error SS_e. Usually the larger the *F*-value, the greater the effect on the performance characteristic due to the change of the process parameter.

The ANOVA module in Qualitek-4 software was used to analyze the impact of process parameters. A review of the "Contribution" column in Table 5 shows that MT contributed the highest percentage (24.88%), followed by MS (16.48%) and BPWR (3.95%).

Table 5 ANOVA table for S/N ratio

Factor	DOF	Sum of Squares	Variance	F-Ratio	Pure Sum	Contribution, %
MS	3	1284.41	428.14	2.51	772.08	16.48
MT	3	1677.78	559.26	3.27	1165.45	24.88
BPWR	3	697.47	232.49	1.36	185.14	3.95
Other error	6	1024.66	170.78	-	-	54.69
Total	15	4684.32	-	-	-	100

The contribution of BPWR was small, so the sum of squares for this parameter was combined with the error, SS_e. This process of disregarding the contribution of a selected parameter and subsequently adjusting the contributions of the other factors is known as pooling. Taguchi recommended pooling factors until the error DoF is approximately half the total DoF of the experiment [29]. A larger DoF for the error term, as a result of pooling, increases the confidence level of the significant parameters. The results of this procedure are summarized in the pooled ANOVA (Table 6).

Table 6 Pooled ANOVA table for S/N ratio

Factor	DOF	Sum of Squares	Variance	F-Ratio	Pure Sum	Contribution, %
MS	3	1284.41	428.14	2.51	772.08	16.48
MT	3	1677.78	559.26	3.27	1165.45	24.88
BPWR	(3)	(697.47)	-	Pooled	(CL=66.03%)	-
Other error	9	1722.13	191.35	-	-	58.64
Total	15	4684.32	-	-	-	100

The DoF for the error is 9, and the DoF for control parameters is 3. Based on the F - distribution Table, at the 0.25 level of significance (75% confidence), the value of F 0.25(3, 12) = 1.56. The computed values of variance ratios F for MT (3.27) and MS (2.51) were greater than the limiting value obtained from the Table. Therefore, a significant influence was seen of MT and MS on DD during the HEBM process. The ANOVA results closely matched the Taguchi equivalents.

3.7. Step 7. Estimation of DD at optimum conditions

In order to estimate the optimum DD of HEBM TiO_2 powder for the maximum result, the significant control parameters with optimum levels were used. The optimum result of DD was carried out using MT at the third level, and MS at the fourth level. The pooled BPWR parameter was not included in the estimation. The estimated mean of the DD was calculated using Equation 3.7:

$$y_{opt} = y_m + \sum_{i=1}^{n} \left(y_j - y_m \right) \quad (3.7)$$

where y_m is the total mean of the DD in accordance with Taguchi's L_{16} OA (Table 3), n is the number of main milling parameters which significantly affected performance, and y_j is the mean measured values for j^{th} milling parameters corresponding to the optimal parameter level. Thus, the DD at optimum conditions was found to be *0.12 line/nm²*.

In statistics, it is customary to represent the values of a statistical parameter as a range within which it is likely to fall, for a given level of confidence. This range is termed the confidence interval (CI) [29]. The CIs of population and confirmation tests were calculated according to Equations 3.8 and 3.9:

$C.I._{POP} = \sqrt{\frac{F_{(\alpha;1,n_2)}V_e}{n_{eff}}}$	(3.8)
$C.I._{CT} = \sqrt{\frac{F_{(\alpha;1,n_2)}V_e}{n_{eff}} + \frac{1}{R}}$	(3.9)
$n_{eff} = \frac{Number\ of\ trials}{1+T_{DoF}}$	(3.10)

where α = 0.1 presents the risk, and n_2 = 9 is the error data regarding the degree of freedom in ANOVA. $F_{(0.1;1,9)}$ is examined as 2.9 [45], which according to the F-ratio table is at 90% CI. T_{DoF} expresses the total number of DoF in accordance with the significant control parameters, and the value was found to be 6. R refers to the sample size of confirmation tests examining DD output, and the data utilized was 3. V_e is the variance of error term (from ANOVA), and this value was found to be 191.35 (Table 6); n_{eff} is the effective number of replications, calculated to be 2.29 (Eq. 3.10). As a result, $CI._{CT}$ and $CI._{POP}$ were analyzed as ±0.06 and ±0.05, respectively. The predicted CIs of population and confirmation tests for DD were calculated via Equations 3.11 and 3.12, respectively:

$y_{opt} - C.I._{CT} < y_{opt} < y_{opt} + C.I._{CT}$	(3.11)
$y_{opt} - C.I._{POP} < y_{opt} < y_{opt} + C.I._{POP}$	(3.12)

The predictive results for the optimal approach in accordance with predicted confidence intervals are tabulated in Table 7.

Table 7 Optimal results for predicted DD

Combination	Predictive DD, line/nm²	Estimated C.I. at 90% Confidence Level
$MS_4MT_3BPWR_4$	0.12	0.06 < y_{opt} < 0.18 (confirmation test)
		0.07 < y_{opt} < 0.17 (population)

3.8. Step 8. Conduction of the confirmation experiment

The final step of the Taguchi method is the confirmation experiment, which is highly recommended to verify the experimental predictions [45]. Confirmation experiments validated the setting factors and levels obtained in our previous calculations. These experiments were conducted using the optimal settings obtained for MS 4^{th} level (600rpm), MT 3^{rd} level (50h),and BPWR 4^{th} level (50:1).

Three confirmation runs were conducted under the optimal conditions. The average TiO_2 DD was found to be *0.13 lines/nm²*. The DD obtained through confirmation experiments were within the 90% CI range (Table 7). Therefore, the results obtained from the confirmation tests reflected successful optimization.

4. Conclusion

In this study, the Taguchi method was used to determine the effects of MT, MS and BPWR on the DD of HEBM TiO_2 powder. The HEBM process was analyzed with the Taguchi $L_{16}(4^3)$ OA. The optimum levels of the control parameters for maximizing the DD were determined using S/N ratios. The optimal conditions for DD were observed at $MS_4MT_3BPWR_4$ (i.e., MS = 600rpm, MT = 50h and BPWR = 50:1). According to the results of ANOVA, it was found that the MT was the most significant parameter for DD, with a percentage contribution of 24.88%, followed by MS (16.48%) and BPWR (3.95%). According to the confirmation test results, the experimentally measured DD was within the 90% CI range. These results showed

that the Taguchi method is a reliable methodology for the reduction of machining time and manufacturing costs in the HEBM of TiO_2 powder. In the future, the results obtained can be used for academic research as well as for industrial applications.

Compliance with ethical standards

Acknowledgments

The authors thank Dr. A. Kossenko, Dr. O. Krichevski and Dr. T. Brieder for assistance with XRD and SEM.

Disclosure of conflict of interest

The authors declare that they have no conflicting interests.

References

[1] Mindess S, Young J and Darwin D (2003). Concrete. Prentice-Hall civil engineering and engineering mechanics series. Prentice Hall.

[2] Fu Q, Zhang Z, Zhao X, Xu W and Niu D (2022). Effect of nano calcium carbonate on hydration characteristics and microstructure of cement-based materials: A review. J. Build. Eng., 50, 104220–104237.

[3] Gowda R, Narendra H, Nagabushan B, Rangappa D and Prabhakara R (2017). Investigation of nano-alumina on the effect of durability and microstructural properties of the cement mortar. Mater. Today Proc., 4(11), 12191–12197.

[4] Reches Y, Thomson K, Helbing M, Kosson D and Sanchez F (2018). Agglomeration and reactivity of nanoparticles of $SiO2$, $T\ iO2$, $Al2O3$, F $e2O3$, and clays in cement pastes and effects on compressive strength at ambient and elevated temperatures. Construct. Build. Mater., 167, 860–873.

[5] Bentur A and Mindess S (2006). Fibre reinforced cementitious composites, second edition. Modern Concrete Technology. Taylor & Francis.

[6] Renuka R, Jayaraman N, Julius A, Palanivel V, Ramachandran V, Pandian R, Luthra U, and Subbiah S (2023). Synthesis, characterization and applications of titanium dioxide nanoparticles. Springer Nature Singapore, Singapore. 339–361.

[7] Pathak SS and Vesmawala GR (2022). Effect of nano $TiO2$ on mechanical properties and microstructure of concrete. Materials Today: Proceedings, 65, 1915–1921. International Conference on Advances in Construction Materials and Structures.

[8] Atta-ur-Rehman A, Qudoos A, Kim H and Ryou J (2018). Influence of titanium dioxide nanoparticles on the sulfate attack upon ordinary portland cement and slag-blended mortars. Materials, 11(3).

[9] Mostafa F, Smarzewski P, El Hafez G. A, Farghali A, Morsi W, Faried A and Tawfik T (2023). Analyzing the effects of nano-titanium dioxide and nano-zinc oxide nanoparticles on the mechanical and durability properties of self-cleaning concrete. Materials, 16(21).

[10] Maggos T, Bartzis J, Liakou M and Gobin C (2007). Photocatalytic degradation of NOx gases using TiO_2-containing paint: A real scale study. Journal of Hazardous Materials, 146, 668–73.

[11] Marien C, Marchal C, Koch A, Robert D and Drogui P (2017). Sol-gel synthesis of TiO_2 nanoparticles: effect of pluronic p123 on particle's morphology and photocatalytic degradation of paraquat. Environmental Science and Pollution Research, 24.

[12] Oh JK, Lee JK, Kim S and Park KW (2009). Synthesis of phase- and shape-controlled TiO_2 nanoparticles via hydrothermal process. Journal of Industrial and Engineering Chemistry. Ind. Eng. Chem., 15, 270–274.

[13] Maury F and Mungkalasiri J (2009). Chemical vapor deposition of TiO_2 for photocatalytic applications and biocidal surfaces. Key Engineering Materials, 415.

[14] Radune M, Lugovskoy S, Knop Y and Kazanski B (2024). Parameter optimization of high energy ball milling process for TiO_2 powder using the Taguchi method. World Journal of Advanced Engineering Technology and Sciences, 12(01), 390–403.

[15] Petrović S, Rožić L, Jović V, Stojadinović S, Grbić B, Radić N, Lamovec J and Vasilić R (2018). Optimization of a nanoparticle ball milling process parameters using the response surface method. Advanced Powder Technology, 29(9), 2129–2139.

[16] Suprapto SRSW and Irawan YS (2019). Parameter optimization of ball milling process for silica sand tailing. IOP Conf. Ser.: Mater. Sci. Eng., 494, DOI 10.1088/1757– 899X/494/1/012073.

[17] Galindez Y, Correa E, Zuleta AA, et al. (2021). Improved Mg–Al–Zn magnesium alloys produced by high energy milling and hot sintering. Met. Mater. Int., 27, 113–1130.

[18] Retamoso C, Escalona N, González M, Barrientos L, Allende-González P, Stancovich S, Serpell R, Fierro JLG and Lopez M (2019). Effect of particle size on the photocatalytic activity of modified rutile sand (TiO_2) for the discoloration of methylene blue in water. J. Photochem. Photobiol. Chem., 378, 136–141.

[19] Suwannaruang T, Kamonsuangkasem K, Kidkhunthod P, Chirawatkul P, Saiyasombat C, Chanlek N and Wantala K (2018). Influence of nitrogen content levels on structural properties and photocatalytic activities of nanorice-like N-doped TiO_2 with various calcination temperatures. Mater. Res. Bull., 105, 265–276.

[20] Song-Jeng H and Matoke PM (2023). High-energy ball milling-induced crystallographic structure changes of AZ61-Mg alloy for improved hydrogen storage. Journal of Energy Storage, 68, doi.org/10.1016/j.est.2023.107773.

[21] Suryanarayana C (2001). Mechanical alloying and milling. Prog. Mater. Sci, 46, 1–184.

[22] Radune M, Lugovskoy S, Knop Y, et al. (2022). Use of Taguchi method for high energy ball milling of CaCO3. Mater Eng, 17(1). https://doi.org/10.1186/s40712-021-00140-8

[23] Hussain Z (2021). Comparative study on improving the ball mill process parameters influencing on the synthesis of ultrafine silica sand: A Taguchi coupled optimization technique. International Journal of Precision Engineering and Manufacturing, 22, 679–688.

[24] Gilbert S, Dalton G, Lucas G, Geovani R and Carlos E (2020). Processing parameters in the ball milling of niobium hydride: An optimization approach. Indian Journal of Engineering & Materials Sciences, 27, 717–723.

[25] Sadeghi B, Shabani A, Heidarinejad A, Laska A, Szkodo M and Cavaliere P (2022). A quantitative investigation of dislocation density in an Al matrix composite produced by a combination of micro-/macro-rolling. J. Compos. Sci., 6(7), 199.

[26] Williamson GK and Hall WH (1953). X-ray line broadening from filed aluminium and wolfram. Acta Met, 1, 22–31.

[27] Ahmed AM, Rabia M and Shaban M (2020). The structure and photoelectrochemical activity of Cr-doped PbS thin films grown by chemical bath deposition. RSC Advances, 10(24), 14458–14470.

[28] Veerappan K, Atul V, Sriramkumar M, Sanath K, Kandasamy J and Yen-Pei F (2019). Investigation of the structural, optical and crystallographic properties of Bi2O6/Ag plasmonic hybrids and their photocatalytic and electron transfer characteristics. Dalton Trans., 48(27), 10235–10250.

[29] Roy R (2001). Design of experiments using the Taguchi approach. Wiley-Interscience Publication.

[30] Fisher RA (1992). Statistical methods for research workers. Springer, New York. 66–70.

[31] Fratila D and Caizar C (2011). Application of Taguchi method to selection of optimal lubrication and cutting conditions in face milling of almg3. Journal of Cleaner Production, 19(6), 640–645.

[32] Phadke MS (1989). Quality engineering using robust design. New Jersey: Englewood Cliffs.

[33] Manni A, Saviano G and Bonelli M (2021). Optimization of the ANNs predictive capability using the Taguchi approach: A case study. Mathematics, 9, 766.

[34] Rizlan Z and Mamat O (2014). Process parameters optimization of silica sand nanoparticles production using low speed ball milling method. Chinese Journal of Engineering, page 4. http://dx.doi.org/10.1155/2014/802459

[35] Hajalilou A, Hashim M, Ebrahimi-Kahrizsangi R, et al. (2014). Parametric optimization of NiFe2O4 nanoparticles synthesized by mechanical alloying. Materials Science-Poland, 32, 281–291.

[36] Kumar GC, Varalakshmi M, Tiwari A and Rajyalakshmi K (2019). Modified Taguchi approach for optimizing the process parameter using the fictitious parameter. Journal of Physics: Conference Series, 1344(1), 012024.

[37] Taguchi G and Konishi S (1987). Orthogonal arrays and linear graphs. Dearborn: American Supplier Institute.

[38] Alyosif B, Uysal T, Aydemir MK and Erdemoğlu M (2023). Contribution of mechanical activation for obtaining potassium chloride from microcline. Mining, Metallurgy and Exploration, 40, 1311–1319.

[39] Xianmei Z, Zhenquan H, Wei J, Fanrong M, Wenju Z, Changai L, Xiangyang H, Guosheng G, Zhaohui H and Minggang X (2023). Mechanism of potassium release from feldspar by mechanical activation in presence of additives at ordinary temperatures. Materials, 17(1), 144.

[40] Yao G, Wang Z, Yao J, Cong X, Anning C and Lyu X (2021). Pozzolanic activity and hydration properties of feldspar after mechanical activation. Powder Technology, 383, 167–174.

[41] Chowdhury GTS and Wu Y (2005). Taguchi's quality engineering handbook. John Wiley & Sons.

[42] Külekcı MK (2013). Analysis of process parameters for a surface-grinding process based on the Taguchi method. Mater. Tehnol, 47, 105–109.

[43] Amoljit G, Amit T and Sanjeev K. (2013). Effect of deep cryogenic treatment on the surface roughness of OHNS die steel after WEDM. International Journal of Applied Engineering Research, 7, 1508–1512.

[44] Edwards A (2005). R.A. Fischer, statistical methods for research workers, First edition (1925). In Landmark writings in Western mathematics 1640-1940. Elsevier Science. 856–870.

[45] Ross P (1996). Taguchi techniques for quality engineering: Loss function, orthogonal experiments, parameter and tolerance design. McGraw-Hill.